PAPER

Low-lying states near the $I^{\pi} = 6^{+}$ isomer in ^{108}Ag

IOP Publishing Journal of Physics G: Nuclear and Particle Physics

J. Phys. G: Nucl. Part. Phys. **43** (2016) 015103 (15pp) doi:10.1088/0954-3899/43/1/015103

Low-lying states near the $I^{\pi} = 6^{+}$ isomer in ^{108}Ag

J Sethi[1], R Palit[1], J J Carroll[2], S Karamian[3,12], S Saha[1], S Biswas[1], Z Naik[4], T Trivedi[1], M S Litz[2], P Datta[5], S Chattopadhyay[6], R Donthi[1], U Garg[7], S Jadhav[1], H C Jain[1], S Kumar[8], D Mehta[9], B S Naidu[1], G H Bhat[10], J A Sheikh[10], S Sihotra[9] and P M Walker[11]

[1] Tata Institute of Fundamental Research, Mumbai 400005, India
[2] US Army Research Laboratory, Adelphi, MD 20783, USA
[3] Joint Institute for Nuclear Research, Dubna 141980, Russia
[4] Sambalpur University, Sambalpur 768019, India
[5] Ananda Mohan College, Kolkata 700009, India
[6] Saha Institute of Nuclear Physics, Kolkata 700064, India
[7] University of Notre Dame, Notre Dame, IN 46556, USA
[8] University of Delhi, Delhi 110007, India
[9] Panjab University, Chandigarh 160014, India
[10] Department of Physics, University of Kashmir, Srinagar 190006, India
[11] Department of Physics, University of Surrey, Guildford, Surrey GU2 7XH, UK

E-mail: palit@tifr.res.in

Received 6 September 2015, revised 21 October 2015
Accepted for publication 23 October 2015
Published 8 December 2015

Abstract

The low-lying states of ^{108}Ag near the $I^{\pi} = 6^{+}$ isomer have been investigated with the ^{11}B + ^{100}Mo reaction at 39 MeV beam energy. We aim at understanding the structure of the states near the isomer and identifying possible isomer depletion paths. From the γ–γ and γ–γ–γ coincidence analysis, spectroscopy of the excited states near the isomer has been carried out to establish new transitions and modification of the previously known level scheme. The present work suggests a total of three possible transitions at energies below 500 keV from the isomer to higher excited levels, whose subsequent decay can branch to the ground state. The spins and parities of these states have been established with angular correlation and polarization measurements. The branching ratios and multipolarities of the associated γ-rays were used in the estimation of the integral cross section for induced isomer depletion via these states. The experimental data have been compared to the results of projected Hartree–Fock calculations to understand the configurations of the levels.

[12] Deceased.

Keywords: isomer, nuclear structure, gamma ray spectroscopy, fusion evaporation reaction

(Some figures may appear in colour only in the online journal)

1. Introduction

Nuclear metastable states with half-lives longer than a few nanoseconds may be found in many nuclides in the nuclear landscape. With the increasing sensitivity of different measuring techniques, a number of new isomers are being discovered with various spectrometers at new accelerator facilities. These isomers provide a tool to study the different nuclear structure models. Furthermore, a wide range of applications of nuclear isomers have been discussed in [1, 2]. In particular, nuclear isomers have the potential to provide material with high energy storage capacity with controlled release of its energy on demand [3–5]. Spectroscopic measurements of the excited states around these isomers are important for evaluation of the depletion pathways of the isomer and the associated rates. The ^{108}Ag nucleus has been a subject of investigation for the study of isomer depletion due to the presence of a long-lived isomer with $T_{1/2} = 438$ y at low spin and high production through the (n, γ) reaction using the stable ^{107}Ag isotope. In odd-odd nuclei, like ^{108}Ag, high-spin isomers with remarkably long lifetimes have been observed due to different two-quasiparticle (2-qp) structures at low excitation energy [6]. The presence of a number of 2-qp structures also makes the search for depletion pathways of the isomers challenging. Our new experimental results from spectroscopic measurements of ^{108}Ag are compared with projected deformed Hartree–Fock (PHF) calculations.

The previously reported works which have discussed the low-lying states of ^{108}Ag are mentioned in [7–13]. The motivation of the present work is to extend knowledge of the level scheme using higher statistics data obtained from the Indian National Gamma Array (INGA) and to ascertain the spin-parity assignments of the concerned low-lying energy levels near the isomeric state. The high spin part of the level scheme has already been reported in a previous publication [14].

2. Experimental details

The ^{108}Ag nucleus was produced in an in-beam experiment using the ^{100}Mo(^{11}B, 3nγ)^{108}Ag fusion evaporation reaction at 39 MeV beam energy. The ^{11}B beam was provided by the Pelletron-LINAC facility at TIFR, Mumbai. The target used was a 10 mg cm^{-2} thick 97% isotopically enriched self-supporting foil of ^{100}Mo. The emitted γ-rays from the de-excitation of the nucleus were detected using INGA consisting of eighteen Compton suppressed clover detectors. The minimum energy threshold of the INGA set up is around 40 keV. The efficiency of the array was obtained by fitting a 7 parameter fitting function (EFFIT) using the RADWARE package [15]. The efficiency of the array was measured for energies ranging from 52 keV to 1408 keV using a mixed ^{152}Eu-^{133}Ba standard radioactive source. Two- and higher-fold clover coincidence events were recorded in a fast digital data acquisition system based on Pixie-16 modules of XIA LLC [16]. The data sorting routine 'Multi pARameter time-stamped based COincidence Search program (MARCOS)', developed at TIFR, sorts the time stamped data to generate $E_\gamma - E_\gamma$ matrices and $E_\gamma - E_\gamma - E_\gamma$ cubes compatible with RADWARE format [15]. These data were used to develop the level scheme. The partial level scheme near the long lived $J^\pi = 6^+$ isomeric state ($T_{1/2} = 438$ y) of ^{108}Ag is shown in figure 1.

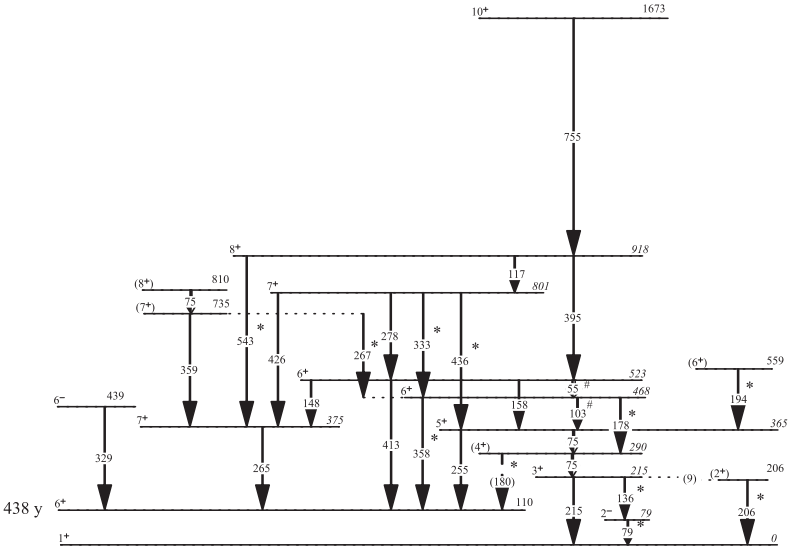

Figure 1. Partial level scheme for ^{108}Ag at low spin relevant for this work. New transitions are marked with an * symbol and the rearranged ones are marked with a # symbol.

The spins and parities of the levels were assigned using directional correlation of oriented nuclei (DCO) ratio analysis and linear polarization measurements of various transitions. Angular distribution measurement for some of the strong transitions were also carried out to determine their multipolarities. In the present geometry of INGA, the clover detectors are placed at different angles in the array, with 3 detectors each at 157°, 140°, 115°, 40°, 2 detectors at 65°, and 4 detectors at 90° with respect to the beam direction.

The intensity of a given γ-ray at an angle θ is given by the following formula,

$$W(\theta) = A_0(1 + a_2P_2(\cos\theta) + a_4P_4(\cos\theta)), \tag{1}$$

where the values of the coefficients a_2 and a_4 depend on the multipolarity of the transition, and $P_2(\cos\theta)$, $P_4(\cos\theta)$ are the Legendre polynomials. The angular distribution was determined for some of the strong transitions of ^{108}Ag. The multipolarities of weaker γ-rays were deduced from the angular correlation analysis [17] using the DCO ratio method for two coincident γ-rays γ_1 and γ_2, given by:

$$R_{\mathrm{DCO}} = \frac{I\left(\gamma_1\right) \text{ observed at } 157^\circ \text{ gated on } \gamma_2 \text{ at } 90^\circ}{I\left(\gamma_1\right) \text{ observed at } 90^\circ \text{ gated on } \gamma_2 \text{ at } 157^\circ}. \tag{2}$$

Here, $I(\gamma_1)$ represents the intensity of γ_1 measured in coincidence with γ_2. In the present geometry of detectors, the DCO ratios obtained with a stretched quadrupole (dipole) gate are 0.5 (1.0) and 1.0 (2.0) for dipole and quadrupole transitions, respectively. The extracted DCO values were obtained by gating on strong stretched $\Delta I = 2$ or $\Delta I = 1$ transitions (see table I). The DCO values of most of the transitions from the higher levels in these bands were obtained with gates on either the 255 keV ($\Delta I = 1$) or the 755 keV ($\Delta I = 2$) transition.

Polarization asymmetry of the gamma-rays was extracted to assign the electric or magnetic nature of the γ-transitions. Each of the four clover detectors present at 90° was used as a Compton-polarimeter to measure the polarization asymmetry of the detected γ-rays [18, 19]. For a Compton-polarimeter, the measured polarization asymmetry Δ of the

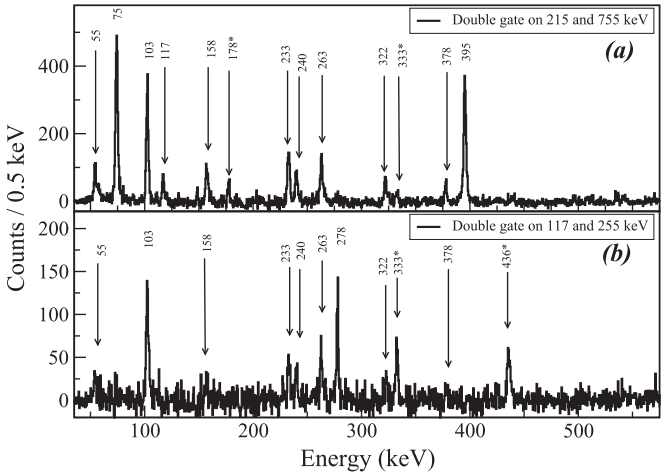

Figure 2. Spectra generated from the double gates on (a) 215 and 755 keV transitions, and (b) 117 and 255 keV transitions, showing the various transitions of the positive parity states near the isomer and also (indicated by asterisks) the newly placed 178, 333 and 436 keV transitions.

transition is defined as

$$\Delta = \frac{a\left(E_\gamma\right)N_\perp - N_\parallel}{a\left(E_\gamma\right)N_\perp + N_\parallel}, \tag{3}$$

where, $N_\perp(N_\parallel)$ is the number of counts of γ transitions scattered perpendicular (parallel) to the reaction plane [18]. The correction factor $a(E_\gamma)$ is a measure of the parallel-to-perpendicular scattering asymmetry within the crystals of the clover detector. For the 90° detectors, this parameter has been found to be 1.00(1) from the analysis of decay data of ^{133}Ba and ^{152}Eu radioactive sources. For linear polarization measurements, two asymmetric matrices corresponding to parallel and perpendicular segments of clover detectors (with respect to the emission plane) along one axis and the coincident γ-rays from the rest of the detectors along the other axis were constructed [20]. Then an integrated polarization directional correlation (IPDCO) analysis was carried out. A positive value of the IPDCO indicates an electric transition while a negative value indicates a magnetic transition.

3. Results

The spectroscopy of the low-lying states of the ^{108}Ag nucleus has earlier been studied from the decay of ^{108m}Ag [7], by using the ^{107}Ag$(n, \gamma)^{108}$ Ag reaction in the works mentioned in [8, 10, 12] and also in the ^{107}Ag(d, p)^{108}Ag reaction [9]. Espinoza-Quiñones *et al* have studied the low spin part of the ^{108}Ag nucleus in the same fusion evaporation reaction as ours and at the same energy but with a smaller number of single crystal HPGe detectors [11]. The present day large Compton suppressed HPGe detector arrays provide us with increased efficiency of γ-ray detection and also provide us with higher-fold coincident data which are more reliable. The present analysis is mostly based on the three- and higher-fold coincident data. We could establish a number of new γ-ray transitions associated with the low-spin structure and the isomeric level with $E_i = 110$ keV and a lifetime of 438 y [21]. The partial

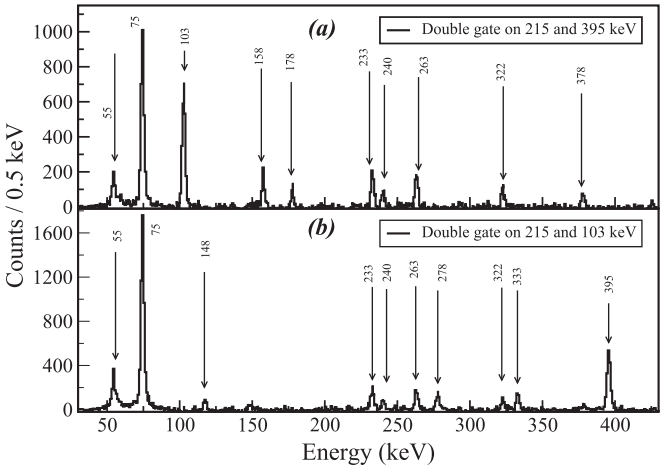

Figure 3. Spectra generated from the double gates on (a) 215 and 395 keV transitions and (b) 215a and 103 keV transitions, showing the various transitions of the positive parity states near the isomer. These two spectra support the rearrangement of the 55 and 103 keV transitions contrary to that reported in the previous level scheme (see [11]).

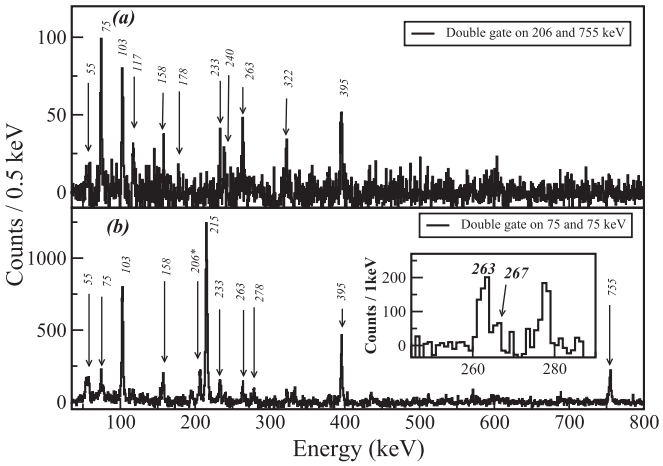

Figure 4. Spectra generated from the double gates on (a) 206 and 755 keV transitions and (b) 75 and 75 keV transitions. The inset spectrum of fig 4 (b) is generated in 75/75 double gate contracted by a factor of two and zoomed in from 240 keV to 290 keV, showing the 267 keV transition from $E_i = 735$ keV to $E_f = 468$ keV.

level scheme of the nucleus in the low spin region near the long lived isomer is shown in figure 1. The γ-transitions marked with an * symbol are the ones which are newly assigned to the level structure of ^{108}Ag and the transitions marked with a # symbol are rearranged in the present work. A brief report of the current work has appeared in [22]. The placements of these new γ-rays are confirmed in various double gated spectra and also supported by the presence of the cross-over transitions. Most of the new transitions are shown in the spectra given in figures 2 and 3. Double gates on the 215 and 755 keV transitions in figure 2(a) show the presence of the new 178 and 333 keV transitions, whereas the spectrum in figure 2(b), with

double gates at 117 and 255 keV, confirms the presence of 333 and 436 keV transitions in the 3 fold coincident data. The γ-energies 233, 240, 263, 322, and 378 keV marked in figures 2–4, decay from the high spin states of a positive parity dipole band feeding the 1673 keV energy level shown in figure 1 [11].

The spectra shown in figures 3(a) and (b) are obtained with the double gates at 215–395 keV and 215–103 keV transitions, respectively. The presence of 158 and 178 keV transitions in the 215–395 keV gated spectrum and their absence in the 215–103 keV gated spectrum, suggests the reordering of the 55 and 103 keV transitions proposed previously [11]. This is further confirmed by the 333 keV transition seen in the 215–103 keV double gated spectrum. In addition, the transition with energy 358 keV is found to decay from the $E_i = 468$ keV level to the isomeric state with $E_f = 110$ keV.

We have also added a few new energy levels at excitation energies of 79, 206, 468, and 559 keV. Though the level energies 79 keV and/or 206 keV have already been observed in the [7–10, 12] in ^{107}Ag(n, γ)^{108}Ag and ^{107}Ag(d, pγ)^{108}Ag reactions. The 79 keV and 206 keV levels have been observed for the first time in a HI fusion evaporation reactions using the coincidence spectroscopy. The parallel placement of 206 keV w.r.t the 215 keV transition is justified by the presence of the 206 keV transition in all the gates above the 215 keV level, but not the 215 keV transition itself. In the double gated spectrum of 206 and 755 keV transitions, the 55-, 75-, 103-, 117-, 178-, 233-, 240-, 263-, 322-, 395 keV transitions have been observed, while the 215 keV is absent (see figure 4(a)). Also, if we look at the double gated spectrum of 75–75 keV in figure 4(b), we see both 206 keV and 215 keV transitions. Therefore, a 206 keV state is placed parallel to the 215 keV transition feeding to the ground state. This also suggests a 9 keV transition decaying from $E_i = 215$ keV to the $E_f = 206$ keV state, which is unobserved in the present experiment, as our set-up has a low energy threshold about 40 keV. The transitions at 79 keV and 136 keV have been placed parallel to both the 206 keV and 215 keV transitions. In figure 4(b), a weak 75 keV transition is observed, which shows that a third 75 keV transition decays from the $J^\pi = 8^+$, 810 keV level to the $J^\pi = 7^+$, 735 keV level, feeding the 75 keV doublet transitions. Also, we do observe a small 267 keV transition in the same spectrum (see inset figure 4(b)) which connects the third 75 keV transition to the 75 keV doublet transitions, decaying from the $E_i = 735$ keV level to the $E_f = 468$ keV level.

A comparison of results from our data with the results from the ^{107}Ag(n, γ)^{108}Ag reaction mentioned in the work by MacMahon *et al* [10] is discussed. The results of MacMahon *et al* are from a very elaborate analysis of a number of measurements of the ^{107}Ag(n, γ)^{108}Ag reaction with various techniques at different experimental facilities and using variety of detectors. The γ-ray energies measured in their experiment were highly precise, but due to the lack of coincidences, they could not place many of the observed transitions in the level scheme. They determined around 65 excited energy states in ^{108}Ag. Focusing on the region of current interest i.e. the low-lying states, they have reported the ground state with $J^\pi = 1^+$, which is consistent with other reported works. The other low spin states which they have assigned have level energies 79.139 keV, 109.440 keV (the isomeric state), 155.876 keV, 193.075 keV, 206.612 keV, 215.382 keV, 294.561 keV, 324.495 keV, 338.419 keV, 364.237 keV, and many more. In our experimental analysis, we could strongly confirm the presence of 79 keV, 110 keV, 206 keV, 215 keV, and 365 keV energy levels. Another 180.552 keV transition is also listed in their table, which was left unplaced [10]. From the current experiment, in the spectrum generated with double gate on 178 keV and 395 keV transitions, a clear peak could not be observed near 180 keV. Therefore, from the sum counts around the 180 keV region, an upper limit on the intensity of a 180 keV transition decaying from $E_i = 290$ keV to $E_f = 110$ keV has been extracted. This possibly can be a pathway through which the isomer could be depleted.

The absence of certain energy levels in our measurement can be explained by the fact that in a typical neutron capture reaction mostly non-yrast states of the nucleus are populated whereas the present measurement is done with a fusion evaporation reaction.

There were certain γ-rays mentioned in the work by MacMahon *et al*, which they observed but could not place in the level scheme due to lack of coincidences with other γ-rays. They observed two γ-ray energies, 74.523 keV and 74.831 keV, which were left unassigned. The presence of these two γ-rays as a 75 keV doublet is confirmed by Espinoza-Quiñones *et al* and also in the present work in a more stringent triple coincidence analysis. Also, a number of other transitions seen in their experiment were left unassigned, out of which 103, 255, 265, 359, 395, 413, and 426 keV transitions have since been placed in the preceding studies of this nucleus and also can be confirmed in our work, whereas 358, 436, and 543 keV transitions have been newly added to the level scheme in the present work. In the yrast band 329 keV and 59 keV transitions were observed but wrongly placed by MacMahon *et al*. The alternative placement of these two γ-rays is in conformity with the present work and also in [11, 13, 14]. The 194 keV transition was placed decaying directly to the ground state by MacMahon *et al*. In the present work, the 194 keV γ-ray is found to be in coincidence with 79 keV, 75 keV, 215, and 255 keV transitions but no coincidences are observed from any of the transitions decaying from higher excited levels to the $E_{\rm i} = 365$ keV level. Therefore, the placement of 194 keV transition, decaying from $E_{\rm i} = 559$ keV to the $E_{\rm f} = 365$ keV level, is suggested.

The measured values of the intensities and the corrected intensities, allowing for the internal conversion coefficients, of the transitions are listed in columns 4 and 5 of table 1, respectively. The values of the internal conversion coefficients are taken from the conversion coefficient calculator BrIcc [23]. The intensities of a few transitions were obtained in the singles spectrum, namely 329 keV, 395 keV, 413 keV, and 755 keV. The intensities of rest of the γ-rays, listed in the table 1, are obtained from the double as well as triple coincident data, normalized relative to the strongest 329 keV transition. At each level, the branching ratios of the γ-rays are carefully extracted and listed in table 2. The spins and parities of the levels were assigned on the basis of IPDCO of oriented nuclei ratio analysis. Also the angular distributions of a few intense and clean γ-rays were obtained from the singles data. Angular distribution measurements were performed using efficiency corrected energy addback spectra of the individual clover detectors at six different angles, namely, 157°, 140°, 115°, 90°, 65°, and 40°. The angular distribution plot for 755 keV transition decaying from $E_{\rm i} = 1673$ keV to $E_{\rm i} = 968$ keV is shown in figure 5. The obtained values of a_2 and a_4 are 0.26(6) and -0.025 (10), respectively. The values of a_2 and a_4 for 755 keV by fitting the experimental data match the values for a pure $\Delta I = 2$ transition as listed in [24, 25]. Therefore, based on angular distribution, DCO ratios and polarization measurement, the present measurements confirm the 755 keV transition to be of stretched E2 character.

The DCO ratios of transitions were mostly extracted with gates at the stretched electric quadrupole 755 keV transition and 255 keV ($\Delta I = 1$) transition. The spectra in figure 6(a), show the 103 keV transition as seen in 157° detectors with a gate on the 755 keV transition in the 90° detectors (red), and the 103 keV transition as seen in the 90° detectors with the gate on the 755 keV transition in the 157° detectors (black) displaying its dipole nature. Similarly, figure 6(b), the spectra for the 395 keV transition is shown in the same gating transition of 755 keV, confirming its quadrupole nature. The polarization asymmetry values could be obtained for a few strong transitions with energies above $\sim$200 keV, looking at the ratio of the parallel to perpendicular scattering of the γ-rays in the 90° detectors, being used as Compton polarimeters. The parallel to perpendicular asymmetry of the two magnetic transitions, namely, 255 and 265 keV is shown in figure 7(a), where it can be clearly seen that there is

Table 1. Table for the spectroscopic observables for the low-lying transitions near the long lived isomeric state. Excitation energies of levels (E_i) in keV, γ-ray energies (E_γ) in keV, relative intensities, branching ratios and multipolarities of the transitions are listed. The errors quoted on the relative intensities are statistical in nature, additional systematic errors ($\sim$10%) are expected.

E_i	J_i^π	$\rightarrow$	J_f^π	E_γ	I_γ	$I_\gamma(1+\alpha)$[a]	Dco[b]	IPDCO
79	2^-	$\rightarrow$	1^+	79.0	>0.49(5)	>0.64(7)	0.66(2) ^{Q}	
206	(2^+)	$\rightarrow$	1^+	206.0	>0.98(8)	>1.04(9)		
215	3^+	$\rightarrow$	2^-	136.0	>0.29(3)	0.31(3)		
215	3^+	$\rightarrow$	1^+	215.2	>6.5(5)	>7.1(6)	0.95(2) ^{Q}	
290	(4^+)	$\rightarrow$	3^+	74.6	>7.3(6)[c]	>14.4(12)	0.52(5)^Q	
290	(4^+)	$\rightarrow$	6^+	(180)	< 0.22(3)	<0.26(3)		
365	5^+	$\rightarrow$	(4^+)	74.8				
365	5^+	$\rightarrow$	6^+	255.2	>10.1(9)	>10.4(9)	0.51(3)^Q	−0.066(23)
375	7^+	$\rightarrow$	6^+	265.2				−0.140(39)
439	6^-	$\rightarrow$	6^+	329.4	100		1.86(1)^D	−0.23(3)
468	6^+	$\rightarrow$	5^+	102.8	8.9(7)	12.4(10)	0.47(3)^Q	
468	6^+	$\rightarrow$	(4^+)	178.0	1.1(1)	1.3(1)	0.97(5)^Q	
468	6^+	$\rightarrow$	6^+	357.8	1.4(1)	1.4(2)	0.52(2)^Q	
523	6^+	$\rightarrow$	6^+	54.7	2.2(2)	18.4(17)[d]	0.91(5)^Q	
523	6^+	$\rightarrow$	7^+	147.7	1.4(1)	1.6(2)	0.66(2)^Q	
523	6^+	$\rightarrow$	5^+	157.6	2.8(2)	3.1(2)	0.52(1)^Q	
523	6^+	$\rightarrow$	6^+	413.1	12.4(9)	12.5(9)	1.02(2)^Q	0.046(12)
559	(6^+)	$\rightarrow$	5^+	194.0	0.89(8)	0.95(9)		
735	(7^+)	$\rightarrow$	6^+	267.0				
735	(7^+)	$\rightarrow$	7^+	359.4				
801	7^+	$\rightarrow$	6^+	278.0	6.3(5)	6.5(5)	0.98(3)^D	−0.081(44)
801	7^+	$\rightarrow$	6^+	333.0	3.6(4)	3.8(4)	1.14(2)^D	−0.042(23)
801	7^+	$\rightarrow$	7^+	426.0	6.9(6)	7.0(8)	1.10(5)^Q	0.057(17)
801	7^+	$\rightarrow$	5^+	435.7	1.5(2)	1.5(2)	0.99(4)^Q	
810	(8^+)	$\rightarrow$	(7^+)	75.0				
918	8^+	$\rightarrow$	7^+	117.0	3.7(3)	5.1(4)	0.57(2)^Q	
918	8^+	$\rightarrow$	6^+	395.7	28.2(23)	28.6(25)	1.92(3)^D	0.073(24)
918	8^+	$\rightarrow$	7^+	543.0	3.1(2)	3.1(2)	0.49(3)^Q	−0.0312(19)
1673	10^+	$\rightarrow$	8^+	755.3	26(3)	26(3)	0.96(4)^Q	0.0990(17)

[a] Values of α are calculated using BrIcc [23].
[b] Nature of the gating transition, Q stands for $\Delta I = 2$ and D for a $\Delta I = 1$ gating transition.
[c] Combined intensity for the 74.6 and 74.8 keV doublet.
[d] Assuming an M1+E2 mixing for calculating the IC coefficient (α) value.

more parallel scattering (black) of the γ-rays compared to the perpendicular scattering (red). However, figure 7(b) shows the electric nature of the transitions at 395 keV and 413 keV, which have more perpendicular scattering compared to parallel scattering of the γ-rays. The values of the measured γ-ray energies, intensities, DCO ratios and polarization asymmetry values are listed in table 1.

The establishment of the spins and parities for the levels is partly on the basis of some previous measurements by other groups. For the ground state, the spin-parity value of 1^+ and for $E_i = 79$, spin-parity value of 2^- are taken from [7] and for the $E_i = 110$ keV, isomeric level, the spin-parity value 6^+ is taken from the nuclear database website [26]. To get an unambiguous value of the $E_i = 290$ keV to $E_f = 215$ keV transition, the DCO ratio of the

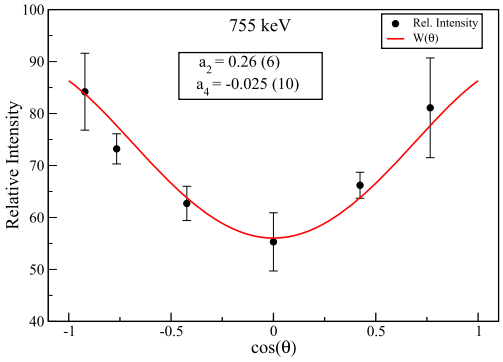

Figure 5. Angular distribution of the 755 keV ($10^+ \rightarrow 8^+$) transition. The solid line represents the fit to the data points.

Table 2. Levels identified as potential intermediate states (IS) for isomer depletion, with transitions and branching ratios describing decays from the higher-lying to lower lying states, although a reversed transition (marked with*) from lower-lying (isomer) to higher-lying (IS) is assumed for the first step in the depletion pathway. The b is the total branching ratio (including conversion) for all decays from the IS other than that directly to the isomer, while $b_{IS\rightarrow g}$ is the part of that branching ratio that ultimately reaches the ground state and ICS is the integral cross section.

E_i	J_i^π	→	J_f^π	E_γ (keV)	b	$b_{IS\rightarrow g}$	$b^\gamma_{m\rightarrow IS}$	ICS (eV b)
290	(4^+)	→	(6^+)	(180)*			<0.030	<0.13
	(4^+)	→	3^+	74.6	0.97(22)	0.97(22)		
365	5^+	→	6^+	255.2*			0.57(7)	25(6)
	5^+	→	(4^+)	74.8	0.41(4)[a]	0.40(9)		
468	6^+	→	6^+	357.8*			0.09(1)	7(1)
	6^+	→	(5^+)	102.8	0.82(9)	0.33(7)		
	6^+	→	(4^+)	178.0	0.09(2)	0.09(2)		
523	6^+	→	6^+	413.1*			0.35(3)	21(4)
	6^+	→	6^+	54.7	0.52(6)	0.22(4)		
	6^+	→	7^+	147.7	0.04(1)	0[b]		
	6^+	→	5^+	157.6	0.09(1)	0.04(1)		

[a] Assuming equal contribution from the 75 keV doublet.
[b] Does not cascade to the ground state, so identically zero.

corresponding 75 keV transition was obtained by gating on the 178 keV ($\Delta I = 2$) transition feeding it from the top. The $E_i = 215$ keV level is assigned $J^\pi = 3^+$ based on the DCO ratio measurement and it is consistent with the value given in [27]. For the $E_i = 206$ keV level, the $J^\pi = 2^+$ spin parity value is taken from the work of MacMahon *et al* [10]. Spins and parities have been assigned to all the other levels based on the DCO and polarization values obtained in the present analysis.

For the 413 keV γ-transition, from $E_i = 523$ keV to isomeric level $E_f = 110$ keV, the DCO ratio and the polarization asymmetry values are found to be 1.02 and 0.046, respectively, with a 755 keV gate (which is an electric quadrupole transition). The polarization asymmetry value and the DCO ratio value indicate that the γ-ray is of mixed magnetic dipole and electric quadrupole nature. Also, the multipolarities of the transitions feeding the 523 keV

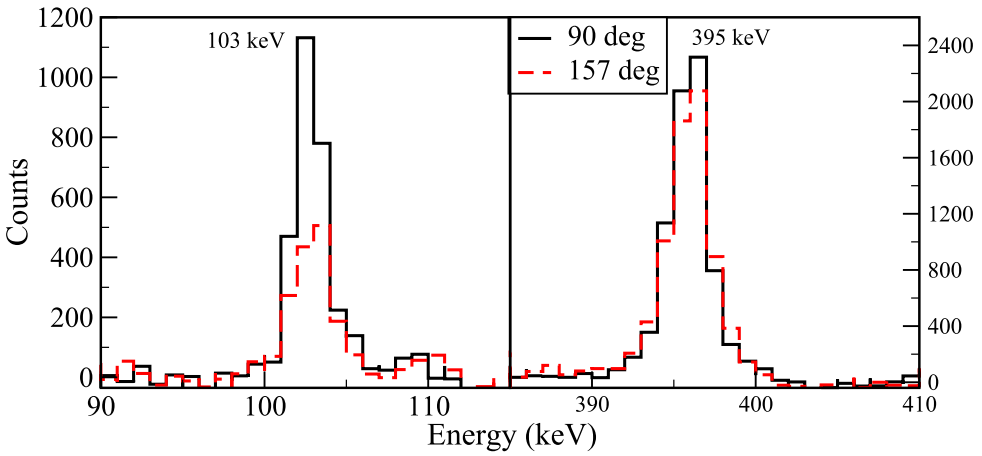

Figure 6. Spectrum projected on 157° detectors with gate on the 755 keV gamma transition in the 90° detectors (in red) and spectrum projected on 90° detectors with gate on the 755 keV in the 157° detectors (in black), showing the $\Delta I = 1$ nature of the 103 keV transition and $\Delta I = 2$ nature of the 395 keV transition.

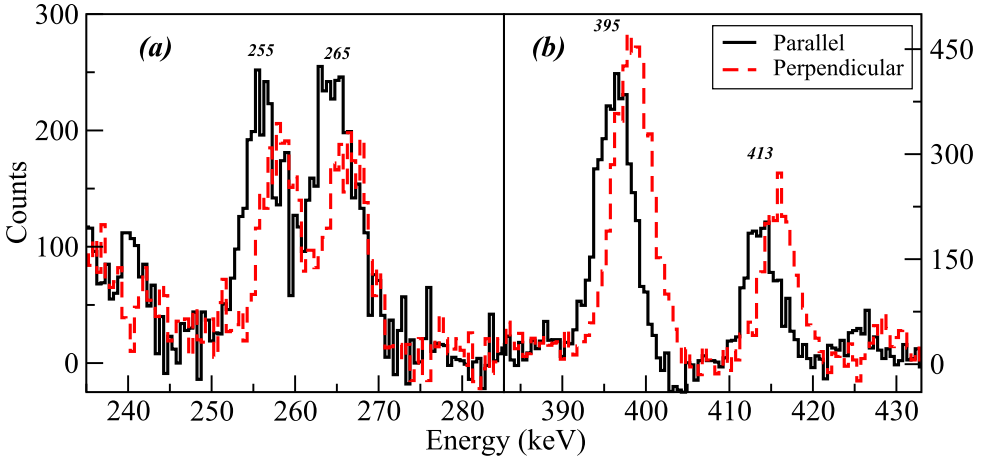

Figure 7. (a) Gated spectra of the perpendicular and parallel Compton scattering in the 90° clover detectors. Higher counts for the 255 and 265 keV transitions in the parallel scattered spectrum indicate their magnetic character while in (b) the opposite trend for the 395 and 413 keV transitions suggest their electric nature. An offset of 3 keV has been introduced between the parallel and perpendicular spectra for clarity.

level i.e., 395 keV and 278 keV, suggest that the level has a $J^{\pi} = 6^{+}$ assignment. We compared the experimental values of DCO ratio and the polarization value of the 413 keV transition to the theoretical values for the various possible multipolarities to understand the nature of the transition. The polarization value (P) of the gamma radiation is calculated as $P = \Delta/Q$, where Δ is the experimental polarization asymmetry value as given in equation (3) and Q is the sensitivity of polarization [19]. The theoretical DCO and polarization values (in accordance with the present geometry of INGA) for different possible $J_i^{\pi} \rightarrow J_f^{\pi}$ assignments of the 413 keV γ-ray, namely $6^{+} \rightarrow 6^{+}$, $7^{+} \rightarrow 6^{+}$, $5^{+} \rightarrow 6^{+}$, $8^{+} \rightarrow 6^{+}$

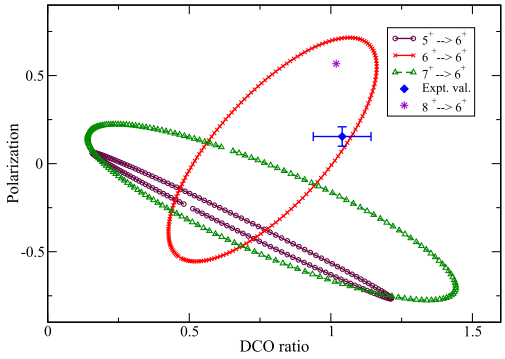

Figure 8. Contour plot for DCO ratio *vs.* polarization value for different possible multipolarities of the 413 keV transition. The different spin sequences are listed in the legend box. The experimental value is found to have the best agreement with the $6^+ \rightarrow 6^+$ contour.

were calculated as a function of mixing ratios. A plot of all these theoretical values along with the experimentally obtained values in figure 8, evidently establish the 413 keV transition to be decaying from $J_i^\pi = 6^+$ to $J_f^\pi = 6^+$.

4. Estimation of integral cross section (ICS) for isomer depletion

Measurements of the intensities and branching ratios of γ-rays, as well as the spin and parity values of the levels are crucial for a better understanding of the possible depletion pathways of the isomer. Isomer depletion and population (or 'photoactivation') via photon absorption require excitation to higher-lying levels typically called intermediate states (ISs). In the present case, potential ISs for depletion of the ^{108m}Ag isomer are identified at 290 keV, 365 keV, 468 keV and 523 keV. For a level to serve as an IS, it must have a gamma branch for decay directly to the isomer, such that this transition could allow excitation of that state from the isomer via photon absorption. A potential IS must also have one or more branches that bypass the isomer and lead to the ground state either directly or by cascade. For those paths, the total branching ratio is required since electromagnetic or electron conversion decays would both lead to the ground state. Table 2 shows relevant information for the potential ISs.

The energy-integrated cross section, or ICS, is used to characterize either isomer depletion or population by photons, since typical photon sources, e.g. bremsstrahlung or inverse Compton scattering, have spectra much broader than that of the resonance excitation functions. The ICS may be written as (similar to equations (4) and (5) of [28]),

$$\mathrm{ICS} = \left(\frac{2J_{\mathrm{IS}} + 1}{2J_m + 1}\right)\left(\frac{\pi\hbar c}{E_{m\rightarrow \mathrm{IS}}}\right)^2 b^{\gamma}_{m\rightarrow \mathrm{IS}}\, b_{\mathrm{IS}} \rightarrow g\ \Gamma_{\mathrm{IS}}, \tag{4}$$

where J_{IS} and J_m are the spins of the IS and isomer, respectively, and $E_{m\rightarrow \mathrm{IS}}$ is the energy of the transition between those levels. The $b^{\gamma}_{m\rightarrow \mathrm{IS}}$ is the branching ratio (without inclusion of electron conversion) for the transition from isomer to IS, while $b_{\mathrm{IS}\rightarrow g}$ is the total branching ratio for all decays of the IS that lead toward the ground state.

In this analysis, Weisskopf estimates are used to determine the widths, Γ_{IS}, of the ISs, since no half-lives are known for those states and Weisskopf estimates are illustrative, very

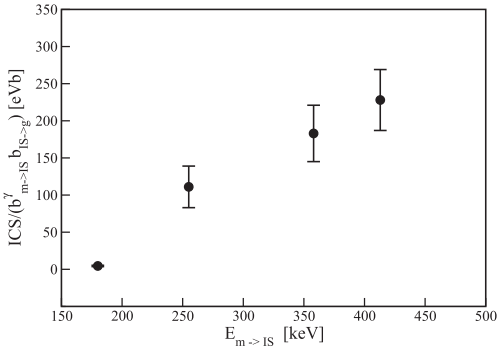

Figure 9. Integral cross section (ICS) per branching ratio product (see equation (4)) for isomer depletion via excitation of intermediate states (IS).

well defined and make fewest assumptions. The single-particle widths for the observed transitions leaving each IS were calculated based on the lowest available multipole and without consideration of multipole mixing. The resulting ICS are given in table 2. The largest values occur for depletion through the intermediates states at 365 keV and 523 keV, being of comparable magnitude.

Clearly the total widths are the principal source of uncertainty in the ICS values, so that detailed conclusions are not possible. It can be noted that the quantity, $\frac{\mathrm{ICS}}{b^{\gamma}_{m\to\mathrm{IS}} b_{\mathrm{IS}\to g}}$ (ICS without the product of branching ratios) increases monotonically with increasing $\mathrm{E}_{m\to\mathrm{IS}}$, as shown in figure 9. However, the variations between the ICS values are significantly larger, resulting from the behavior of the branching ratio factor, as determined from the measured gamma intensities. This emphasizes the critical importance of nuclide-specific information (branching ratios from individual levels) in determining the magnitude of ICS for isomer depletion and the difficulty in drawing broad systematic inferences. It is just for this reason that null results for depletion of one isomer of one nuclide [4, 5] for excitation in one energy range cannot be taken to preclude depletion at other energies for other isomers. We note that future experiments could directly determine the lifetimes of the ISs. Also, the level widths could be determined via equation (4) from excitation functions for photon-depletion experiments conducted using tunable bremsstrahlung sources, since the branching ratios from the IS have now been determined. However, such experiments have not yet been conducted.

5. Projected Hartree–Fock calculations

PHF calculations have been carried out to understand the different configurations involved for the low-lying states of ^{108}Ag near the isomer. A nuclear Hamiltonian that consists of the single particle and two-body interaction terms has been considered for the derivation of the deformed HF equation [29, 30]. The surface delta interaction with strength $V_{\mathrm{pp}} = V_{\mathrm{np}} = V_{\mathrm{nn}} = 0.3$ MeV is taken as the two-body residual interaction among the active nucleons. The spherical single particle states used for PHF calculations are $3s_{1/2}$, $2d_{3/2}$, $2d_{5/2}$, $1g_{7/2}$, $1g_{9/2}$, $1h_{9/2}$, and $1h_{11/2}$ with energies 3.654, 3.288, 0.0, 0.64, −6.541, 5.033 and 0.8 MeV, respectively for protons and $3s_{1/2}$, $2d_{3/2}$, $2d_{5/2}$, $1g_{7/2}$, $2f_{7/2}$, $1h_{9/2}$, and $1h_{11/2}$ with energies −4.848, −4.577, −6.4, −6.0, 1.592, 2.106, and −3.2 MeV, respectively for neutrons. The model space considered

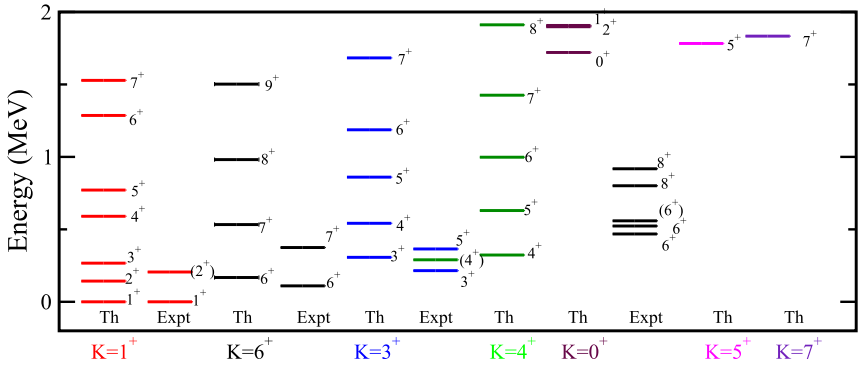

Figure 10. Comparison of the energy levels of the positive parity states near the isomer at low excitation energy with the PHF calculations based on different configurations.

Table 3. Intrinsic configurations used for calculations.

		Particle configuration	
Index	K^{π}	Proton	Neutron
C1	1^+	$7/2\ ^+(g_{9/2})$	$-5/2^+(g_{7/2})$
C2	6^+	$7/2\ ^+(g_{9/2})$	$5/2^+(g_{7/2})$
C3	3^+	$7/2\ ^+(g_{9/2})$	$-1/2^+(d_{3/2})$
C4	4^+	$7/2\ ^+(g_{9/2})$	$1/2^+(d_{3/2})$
C5	0^+	$5/2\ ^+(g_{9/2})$	$-5/2^+(g_{7/2})$
C6	5^+	$5/2\ ^+(g_{9/2})$	$5/2^+(g_{7/2})$
C7	7^+	$9/2\ ^+(g_{9/2})$	$5/2^+(g_{7/2})$

here is outside the inert spherical core with $Z = 40$ and $N = 50$. The prolate HF mean field solution is energetically favored for ^{108}Ag giving the deformation as $\beta = 0.15$. Axial symmetry of the Hartree–Fock field is assumed in the calculation. The intrinsic configurations $|\phi_K\rangle$ used in the present calculations are listed in table 3. The rotational states built on each of these seven configurations after band mixing calculation are shown in figure 10 along with the measured levels for comparison. The low-lying positive parity states in ^{108}Ag have contributions from $\pi\ g_{9/2}$ and $\nu\ g_{7/2}$ orbitals which are near the Fermi surface. Here, we have mixed all the configurations listed in the table 3 for the study of the positive parity states. In our band mixing calculation, we observe that except for the $K = 1^+$ and $K = 3^+$ configurations, the rest are mixed very little with other configurations (states are arround 95% of the given configuration). For the $K = 1^+$ and $K = 3^+$ configurations, the mixing increases from 3% at $I^{\pi} = 3^+$ to about 50% at $I^{\pi} = 8^+$. In Our band mixing calculation, the calculated energy of $I^{\pi} = 1^+$ state mainly originating from configuration C1 is normalized to the ground state since this state is found to be the lowest in energy after mixing calculations (this state is 99.76% of C1 and contribution of C6 is 0.24%).

The excitation energy of the 6^+ isomeric state at 110 keV is fairly well reproduced within 58 keV with configuration C2 (the other five configurations contribute 0.64%). The lowest $I^{\pi} = 7^+$ state after band mixing (mainly based on configuration C2, with 4% contribution to this state from the rest of the configurations) is higher than the measured 7^+ state at 375 keV excitation. The g-factor of the 215 keV level was reported as $+1.301(11)\ \mu_N^2$ [31]. This

measured value is reproduced with $\pi g_{9/2}(7/2) \otimes \nu d_{3/2}(-1/2)$ configuration (C3) which gives a value of 1.262 $\mu_N{}^2$ (mixing of the two other configurations (C1 and C5) to this state is 3%). The measured 4^+ state decaying to the 3^+ state at 215 keV is found to be more bound than the 4^+ state of configuration C3. This lowest $I = 4^+$ state is mainly built on configuration C4 (99.9%) and looks more probable for the 4^+ state at 290 keV. The 5^+ and 6^+ states mainly originating from configuration C4 in band mixing caculations are lower in energy compared to the states of the same spin originating from other configurations mentioned in the table 3. Therefore, most likely, the lowest 5^+ and 6^+ states can be attributed to configuration C4 (contributions of C4 to these states are 99.9% and 99.8%, respectively).

6. Conclusion

The low spin region of the ^{108}Ag nucleus, close to the very long lived isomeric level ($E_i = 110$ keV, $T_{1/2} = 438$ y), has been studied in an in-beam fusion evaporation reaction. A good number of new γ-rays have been identified and placed in the level scheme. The identification of the new levels and γ-transitions bypassing the isomer has made it possible to estimate the ICSs for the isomer depletion. The intensities of the γ-rays, branching ratios, spins and parities of the energy levels have also been assigned to the newly placed levels and confirmed for the already known part of the level scheme. A comparison of the present results to the work of MacMahon *et al* has been made. A few agreements and also disagreements with their (n, γ) data results have been discussed. The current measurement will improve the estimation of the cross section for induced isomer depletion through the low-lying states. PHF calculations have been performed to understand the configurations in the low spin region and the calculated energy levels have been compared to the experimental data.

Acknowledgments

The authors would like to thank the members of INGA Principal Investigating Coordination Committee and INGA collaboration for making the detectors available. The staff at TIFR-BARC Pelletron-LINAC Facility is gratefully acknowledged for the smooth operation of the accelerator. J J Carroll would like to thank C J Chiara for some useful discussions. This work was partially supported by the Department of Science and Technology, Government of India under Grant No. IR/S2/PF-03/2003-II, the US National Science Foundation (Grant No. PHY-1068192), and the UK Science and Technology Facilities Council under grant No. ST/L005743/1.

References

[1] Walker P M and Dracoulis G D 1999 *Nature* **399** 35
[2] Walker P M and Carroll J J 2007 *Nucl. Phys. News* **17** 11
[3] Carroll J J 2009 *AIP Conf. Proc.* **1109** 44
[4] Ahmad I *et al* 2001 *Phys. Rev. Lett.* **87** 072503
[5] Carroll J J *et al* 2009 *Phys. Lett.* B **679** 203
[6] Liu H L, Xu F R, Xu S W, Wyss R and Walker P M 2007 *Phys. Rev.* C **76** 034313
[7] Kistner O C and Sunyar A W 1966 *Phys. Rev.* **143** 918
[8] Bolotin H H and Namenson A I 1967 *Phys. Rev.* **157** 1131
[9] Brient C E, Riley P J, Seitz H and Sen S 1972 *Phys. Rev.* C **6** 1837
[10] MacMahon T D *et al* 1985 *J. Phys. G: Nucl. Phys.* **11** 1231
[11] Espinoza-Quiñones F R *et al* 1995 *Phys. Rev.* C **52** 104

[12] Zanini L *et al* 2003 *Phys. Rev.* C **68** 014320
[13] Liu C *et al* 2011 *Int. J. Mod. Phys.* E **20** 2351
[14] Sethi J *et al* 2013 *Phys. Lett.* B **725** 85
[15] Radford D C 1995 *Nucl. Instrum. Methods* A **361** 297
[16] Palit R *et al* 2012 *Nucl. Instrum. Methods* A **680** 90
[17] Krämer-Flecken A *et al* 1989 *Nucl. Instrum. Methods* A **275** 333
[18] Starosta K *et al* 1999 *Nucl. Instrum. Methods* A **423** 16
[19] Palit R *et al* 2000 *Pramana* **54** 347
[20] Lakshmi S *et al* 2005 *Nucl. Phys.* A **761** 1
[21] Schrader H 2004 *Appl. Radiat. Isot.* **60** 317
[22] Sethi J *et al* 2015 *Acta Phys. Pol.* B **46** 703
[23] Kibedi T, Burrows T W, Trzhaskovskaya M B, Davidson P M and Nestor C W Jr 2008 *Nucl. Instrum. Methods* A **589** 202
[24] Diamond R M *et al* 1966 *Phys. Rev. Lett.* **16** 1205
[25] Newton J O *et al* 1967 *Nucl. Phys.* A **95** 357
[26] Blachot J 2000 *Nucl. Data Sheets* **91** 135
[27] Bertschat H *et al* 1974 *Nucl. Phys.* A **229** 72
[28] Belic D *et al* 2001 *Nucl. Instrum. Methods* A **463** 26
[29] Naik Z and Praharaj C R 2003 *Phys. Rev.* C **67** 054318
[30] Deo A Y *et al* 2009 *Phys. Rev.* C **79** 067304
[31] Hattori T, Adachi M and Taketani H 1976 *J. Phys. Soc. Japan* **41** 1830